

Article

# Transcriptome analysis of ovaries in mice with premature ovarian failure after treatment with Zishen Yutai pills

Zifan Song<sup>1,†</sup>, Kuangyu Song<sup>2,†</sup>, Jing Zhang<sup>1</sup>, Lin Li<sup>3</sup>, Yuanqiao He<sup>4</sup>, Jia Hu<sup>1,\*</sup>

- <sup>1</sup> Department of Obstetrics and Gynecology, The First Affiliated Hospital of Nanchang University, Nanchang, Jiangxi 330006, China
- <sup>2</sup> School of Basic Medical Sciences, Jiangxi Medical College, Nanchang University, Nanchang, Jiangxi 330006, China
- <sup>3</sup> Department of Reproductive, Reproductive Hospital Affiliated to Jiangxi University of Traditional Chinese Medicine, Nanchang, Jiangxi 330110, China
- <sup>4</sup> Jiangxi Province Key Laboratory of Laboratory Animal, Nanchang, Jiangxi 330031, China
- \* Corresponding author: Jia Hu, hujia3009@126.com
- † These authors contributed equally to this work and are co-first authors.

#### CITATION

Song Z, Song K, Zhang J, et al. Transcriptome analysis of ovaries in mice with premature ovarian failure after treatment with Zishen Yutai pills. Journal of Biological Regulators and Homeostatic Agents. 2025; 39(3): 3677. https://doi.org/10.54517/jbrha3677

#### ARTICLE INFO

Received: 12 May 2025 Revised: 3 July 2025 Accepted: 31 July 2025

Available online: 23 October 2025

#### COPYRIGHT



Copyright © 2025 by author(s). Journal of Biological Regulators and Homeostatic Agents is published by Asia Pacific Academy of Science Pte. Ltd. This work is licensed under the Creative Commons Attribution (CC BY) license.

https://creativecommons.org/licenses/by/4.0/

Abstract: Premature ovarian failure (POF) is a critical cause of female infertility, influencing not only reproduction but also life quality. Among the many treatments of POF, hormone replacement therapy is the most commonly adopted. However, it increases the risk of gynecologic tumour formation as well as the severity of cardiovascular and cerebrovascular disorders. Zishenyutai Pill (ZSYTP) is a traditional Chinese patent medication that has been widely used to treat infertility in China, while its underlying mechanism and therapeutic targets on POF remains unknown. To investigate this, we used 4-vinylcyclohexene diepoxide to build POF mouse model, and treated with ZSYTP. Ovaries were collected for histopathological observation, apoptosis assessment and RNA-seq analysis. Results showed that ZSYTP treatment not only decreased atretic follicles, but also increased primary and secondary follicles. In comparison to Model group, ZSYTP group had a significantly lower apoptotic index. Analysis based on differentially expressed genes (DEGs) between Normal and Model group revealed that the immunological response, cell-cell adhesion, and phagosome pathways were most closely associated with the development of POF, while the employment of ZSYTP could ameliorate them. RT-qPCR demonstrated that ZSYTP treatment downregulated the expression of H2-Ab1, H2-Eb1, and H2-Aa, which play multiple and vital roles in immune response. In conclusion, ZSYTP can alleviate ovarian damage of POF mice possibly by downregulating immune response, cell-cell adhesion, and phagocytic pathways.

**Keywords:** Zishen Yutai Pills; Chinese medicine; premature ovarian failure; RNA-seq; transcriptomics

#### 1. Introduction

Premature ovarian failure (POF) is characterized by ovarian hypofunction before age 40, manifesting as low oestrogen and elevated gonadotropins, and represents a leading cause of female infertility [1]. According to European Society of Human Reproduction and Embryology (ESHRE), the incidence of POF and early menopause has reached 3.5%, markedly higher than the estimated 1% in 1986 [2,3]. As POF's prevalence rises, there is growing worry focusing on its series of health problems. Infertility, menopause, and other serious disorders like cognitive decline, osteoporosis, and cardiovascular disease are just a few of the difficulties faced by women with POF [1]. Unfortunately, the etiology of POF is complex and multifactorial, including genetic predisposition, autoimmune dysregulation, pharmacologic insults, and

environmental factors, posing challenges for timely diagnosis and effective treatment [4,5].

Current first-line interventions for POF include ovulation induction and hormone replacement therapy (HRT) [6]. Although HRT efficiently restores the menstrual cycle and alleviates patients' psychological burden, its long-term use carries increased risks of breast and ovarian cancers [7,8]. In response, researchers have explored novel therapeutic approaches, including immunomodulation, gene therapy, stem cell transplantation, and acupuncture, with promising but preliminary results that warrant further validation [9–13]. Traditional Chinese medicine (TCM), with its long history of gynecological applications in China, offers an alternative reservoir of botanical formulas. Among these, many botanical compounds and prescriptions have been employed to treat infertility and menstrual irregularities in routine practice [14], spurring efforts to find promising TCM formulas capable of substituting HRT to treat POF.

Zishen Yutai pill (ZSYTP), a well-known Chinese patent medicines which was first formulated by Professor Yuankai Luo in the early 1960s and commercially available since 1983, is widely used in China to treat recurrent abortion, infertility and other reproductive disorders. Over four decades of clinical use have demonstrated its safety and efficacy. Recent studies indicate that ZSYTP can also improve ovarian reserve by lowering follicle-stimulating hormone (FSH) and raising serum oestrogen, thereby ameliorating hypoestrogenic symptoms [15,16]. Color Doppler ultrasonography further shows that the administration of ZSYTP also stimulated follicle growth and improved ovarian stromal blood flow, resulting in higher clinical pregnancy and live birth rate [17]. However, the underlying mechanism of ZSYTP on POF treatment remains unclear.

Animal models established by chemical ovotoxicants are fundamental for POF research. 4-vinylcyclohexene diepoxide (VCD), a metabolite of 4-vinylcyclohexene used in the production of rubber, agriculture chemicals, fire retardants, and aromatics, exhibits marked ovarian toxicity [18]. VCD not only accelerates apoptosis of primordial and primary follicles, but also replicates POF-associated complications such as depression and osteoporosis in rodents, making it an efficient ovarian toxin to construct POF animal models [19-22]. Mechanistically, VCD triggers oocyte apoptosis and granulosa cell degeneration, leading to primordial follicle atresia akin to human POF [23,24]. Thus, we consider VCD as a proper inducer to mimic POF caused by toxic chemicals exposure. In our previous study, we found that ZSYTP might cure cyclophosphamide (CTX)-induced POF mice by regulating several signaling pathways and immune response [25]. Herein, we employ a VCD-induced POF mouse model coupled with RNA sequencing (RNA-Seq) analysis to comprehensively assess ZSYTP's therapeutic effects and mechanisms at the transcriptomic level. By comparing distinct POF models, we intent to determine whether ZSYTP exerts its benefits through shared molecular mechansims regardless of the underlying cause.

### 2. Materials and methods

#### 2.1. Animals

We bought eight-week-old, healthy female C57BL/6 mice from Zhejiang Weitong Lihua Experimental Animal Technology Co., Ltd. in Zhejiang, China. Mice were raised in a controlled environment with a 12-h light-dark cycle and a temperature of  $23 \pm 3$  °C with unrestricted access to food and water. Before any interventions, the mice were allowed to acclimate for a week. Every animal experiment was carried out in accordance with Nanchang Royo Biotech Co., Ltd.'s Institutional Animal Care and Use Committee Guide (IACUC Issue No: RYE2021012601).

### 2.2. Chemicals and reagents

VCD was acquired from Shanghai Macklin Biochemical Technology Co., Ltd. (Shanghai, China). It is an isomer mixture with a purity of about 96%. The VCD working solution (1.094 g/mL) was created in accordance with the previous study [25].

ZSYTP was acquired from Guangzhou Baiyunshan Zhongyi Pharmaceutical Co., Ltd (Guangzhou, China). The terminal deoxynucleotidyl transferase dUTP nick endlabeling (TUNEL) Assay Kit-HRP-DAB was acquired from Wuhan Boster Biological Engineering Co., Ltd. (Wuhan, China), and the anti-caspase-3 antibody was acquired from Abcam (London, UK). CLIA kits for measuring FSH and Anti-Müllerian Hormone (AMH) were bought from Wuhan cloud-clone Technology Co., Ltd. (Wuhan, China).

#### 2.3. Model construction and treatment

Eight-week-old female C57BL/6 mice were randomly assigned to Normal, Model, and ZSYTP group with 15 mice per group. Every day for 20 days, the model and ZSYTP groups received daily intraperitoneal injections of VCD (80 mg/kg/day), while the Normal group received the same volume of sesame oil.

The dosage of ZSYTP was established according to the dosage exchange formula from humans to mice (experimental dose: clinical dose = 1:9.1). Mice in ZSYTP group were intragastrically administered ZSYTP solution, while Model and Normal group received identical amount of distilled water, A standard administration cycle consists of six days of continuous dosing separated by one day off. After four administration cycles, all mice were sacrificed to collect ovarian tissues and serum samples for additional examination.

#### 2.4. Hormone assay

Chemiluminescent immunoassay was used to assess FSH and AMH levels in serum, referring to the manufacturer's instructions. All standards and serum samples were thoroughly diluted with PBS to the desired concentration. Next, 50  $\mu L$  of either sample or standard was pipetted into microwell plates covered with monoclonal antibodies of FSH or AMH. The microwell plate was treated with 50  $\mu L$  of detection solution A and incubated for one hour at 37 °C. After incubation, the plates were washed three times with PBS solution then added 100  $\mu L$  of detection solution B to each well and incubated for 30 min at 37 °C. After five washes with PBS, 100  $\mu L$  of substrate was applied to each well and incubated at 37 °C for 10 min. The relative optical units of FSH and AMH were detected by chemiluminescence equipment.

### 2.5. Hematoxylin and eosin staining

Mice ovarian tissues were fixed in 4% paraformaldehyde at 25 °C for 12 h before being dehydrated with gradient ethanol (70%, 80%, and 95% twice, and 100% twice), followed by xylol washing. The entire ovary was embedded in paraffin and sectioned into 5  $\mu$ m slices then preserved at 4 °C for later analysis. Hematoxylin and eosin (H&E) staining was used to examine the histomorphology of ovarian tissue sections. For each group, the mean value of the number of follicles at each stage was determined using three consecutive sections with the largest cross-sectional area per mouse. The statistical results were quantified using ImageJ software.

#### 2.6. TUNEL staining

TUNEL staining was utilized for determining apoptosis in ovarian samples. Slides were rehydrated in ethanol and xylene gradients then incubated for 20 min with 1:100 protease K solution. After that, the slides were treated with 3% H2O2 containing methanol for 5 min to inactivate endogenous peroxidase. The slides were covered with terminal deoxynucleotide transferase (TdT) equilibration buffer for 30 min. Subsequently, the samples were added to the TdT labeling reaction mix and incubated in a humidified chamber for 1.5 h at 37 °C. The labeling reaction was terminated by adding stop buffer. After blocking for 10 min, the specimens were incubated in diluted conjugate (1:500) for 30 min in humidified chamber, then stained in diaminobenzidine solution for 15 min. The slices were counterstained with hematoxylin for 3 min then rinsed in 100% ethanol and 100% xylene successively. The slices were then mounted with glass coverslips and transferred to a light microscope to examine TUNEL-positive cells.

#### 2.7. Immunohistochemistry

The paraffin slices of ovarian tissue were deparaffinized with dimethylbenzene and graded ethanol, and the remaining solutions were removed by washing with PBS. The endogenous peroxidase in the tissue was inactivated using a 10%  $H_2O_2$  solution. The nonspecific binding locations were coated with 5% BSA for 30 minutes. The slices were then incubated with rabbit anti-caspase-3 (1:500) overnight at 4 °C. The following morning, they were rinsed with PBS three times before incubating with secondary antibody for 50 min at 37 °C. Following a rinse with PBS, DAB was added to visualize positive staining, and the cell nuclei were stained with hematoxylin solution. The positive rate was determined in three random fields at  $\times$  200 magnification using optical density. For TUNEL and immunohistochemistry assay, four consecutive histological sections with the largest cross-sectional area were selected to represent a whole ovary. Each slice was regarded as an independent sample for analysis. To calculate the average optical density (AOD) of caspase-3, four non-overlapping areas of each slice were selected randomly.

#### 2.8. Bulk RNA sequencing

Detailed protocol of transcriptome sequencing was described in our previous study [26]. Briefly, using the TRIzol method to isolate RNA from unilateral ovary of each mouse. Then perform RNA sample quality analysis on Fragments Analyzer with

RNA analysis kit (15nt; DNF-471; Agilent Technology, Palo Alto, United States). The RNA samples were diluted into appropriate concentration as the library construction guideline recommended to establish sequencing library. After RNA thermal denaturation, add magnetic beads coated with oligonucleotides (dT) to enrich poly(A)-tailed mRNA. Fragment the obtained mRNA with fragmentation reagent, then use the primer N6 to synthesize double-strand cDNA. After performing End repair, A-tailing, and adaptor connection, the cDNAs were amplified and then circularized by PCR to produce DNA nanoballs (DNBs) through rolling circular cycle amplification. Then, the high-quality DNBs were loaded into the patterned nanoarray and sequenced on DNBSEQ platform. Raw sequencing data were filtered with FastQC to conduct quality control. After filtering, the clean data was mapped to the reference genome using HISAT2 (v2.1.0) [27]. The differential expression analysis was conducted using DESeq2 R package (v. 1.44.0) based on counts [28]. Differentially expressed genes (DEGs) were defined as those with *q*-value < 0.05 and fold change > 2.

#### 2.9. GO and KEGG analyses of DEGs

After obtaining DEGs between each two groups, Gene Ontology (GO) and Kyoto Encyclopedia of Genes and Genomes (KEGG) enrichment analyses were performed using the DAVID database (https://david.ncifcrf.gov/home.jsp) to further investigate the therapeutic mechanism of ZSYTP on POF [29]. A p-value threshold OF < 0.05 was set to determine significance. The top 10 GO terms with the highest Enrichment Score and the top 15 KEGG pathways with the lowest p-value score were selected for visualization.

#### 2.10. Real-time fluorescence quantitative validation of DEGs

Based on the results of RNA-Seq, real-time fluorescence reverse transcription-quantitative polymerase chain reaction (RT-qPCR) was performed for *s100a8*, *cxcl13*, *cxcl5* and *caspase3*. RNA of ovarian tissue was extracted by TRIzol. The PrimeScript FAST RT reagent Kit with gDNA Eraser (Takara, RR092A) was used to reverse the extracted RNA into cDNA, and *Gapdh* was used as the reference gene. Real-time fluorimetric analysis was performed using TB Green Premix EX Taq II (Takara, RR820A) according to the instructions. Primer information is provided in **Table S1**. The primers were synthesized by Shenggong Bioengineering Co., Ltd (Shanghai, China).

### 2.11. Statistical analysis

Data from animal experiments were expressed as mean  $\pm$  standard deviation. The statistical analysis and graph plotting were done with GraphPad Prism 8 software. Student's *t*-test was used for the statistical difference between the two groups, and one-way analysis of variance (ANOVA) was used for comparisons involving two or more groups, followed by the LSD post hoc test. *p*-value < 0.05 were considered statistically significant.

#### 3. Results and discussion

# 3.1. ZSYTP decreased the FSH level and increased the AMH level of POF mice

Elevated FSH and reduced AMH serum levels are crucial characteristic of POF. After VCD exposure, the level of FSH significantly increased whereas AMH decreased, corresponding with the hormone level change of POF (*p*-value < 0.05; **Figure 1A, B**). Encouragingly, the administration of ZSYTP markedly recovered the FSH and AMH levels which were both nearly equivalent to the Normal group (*p*-value < 0.05). These findings suggested that ZSYTP remarkably improved the serum hormone levels of VCD-induced POF mice.

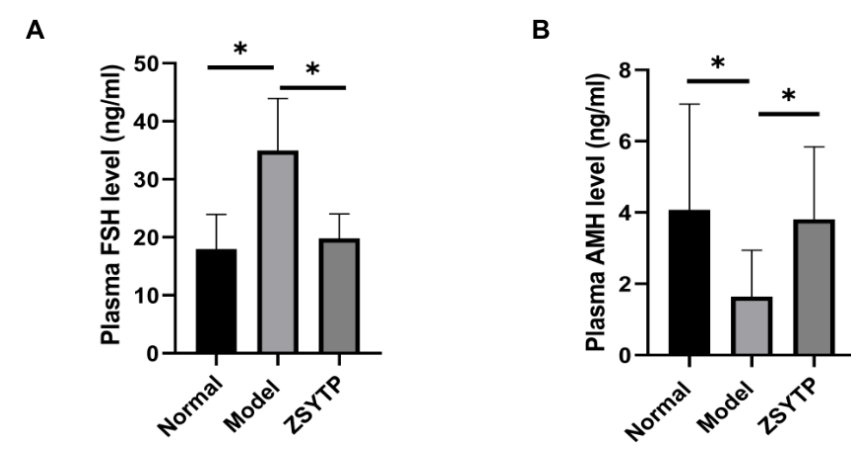


**Figure 1.** Endocrine level measurement: **(A)** The level of FSH in each group; **(B)** The level of AMH in each group. \*p-value < 0.05. AMH, anti-mullerian tube hormone; FSH, follicle-stimulating hormone.

#### 3.2. ZSYTP protected follicle quantity and quality

The histological changes of ovaries and follicular count depict ovarian reserves. As shown by H&E staining, ovaries of Normal group had normal size, containing plentiful follicles of various stages with diverse size in the cortical area (**Figure 2A**). By contrast, ovaries in the Model group appeared much atrophic and formless, with significantly reduced primordial, growing and antral follicles and increased atretic follicles (*p*-value < 0.05; **Figure 2B–F**). In addition, most follicles in Model group were atretic, showing a smaller volume of follicles compared to the Normal group. These results further confirmed our successful establishment of a VCD-induced POF mice model.

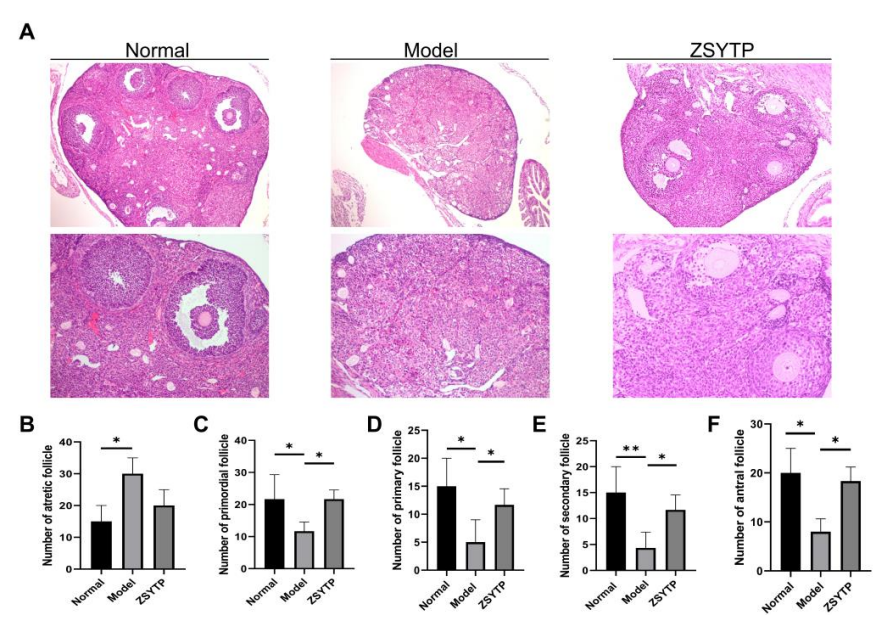


**Figure 2.** Ovarian histopathology and follicle count: **(A)** H&E staining of ovary; **(B–F)** The number of f ovarian follicle in each stage. H&E, hematoxylin and eosin; ZSYTP, Zishen yutai Pill.

Compared with the Model group, the total ovarian histomorphology and follicle quality were visibly improved in the ZSYTP group. More growing follicles were observed in the ovarian cortex (**Figure 2A**). Moreover, ZSYTP significantly recovered the number of primordial, primary, secondary and antral follicles reduced by VCD exposure (p-value < 0.05), despite no significant difference in the number of atretic follicles (p-value = 0.1089; **Figure 2B**). These results demonstrated that ZSYTP could protect ovarian reserve in VCD-induced POF mice.

# 3.3. ZSYTP mitigated ovarian apoptosis without altering whole-ovary apoptosis protein levels

As the cell apoptosis occupies an important role in the development of POF, it is essential to evaluate the apoptotic level of ovarian tissue in POF mice. Follicle apoptosis was quantified by counting the number of apoptotic cells in follicles within the field of view of the microscope (four slices per ovary; five ovaries per group). Follicles were considered as TUNEL-positive if more than 5% cells stained positive. Atretic follicles were considered as 100% TUNEL-positive. The apoptotic index was calculated as the ratio of TUNEL-positive follicles to total follicles. As depicted in **Figure 3A**, the concentration of TUNEL-positive cells was the highest in Model group. Consistently, the apoptotic index of Model group was significantly increased compared with the Normal group, while the administration of ZSYTP alleviated the proportion of TUNEL-positive cells in follicles (*p*-value < 0.05; **Figure 3B**).

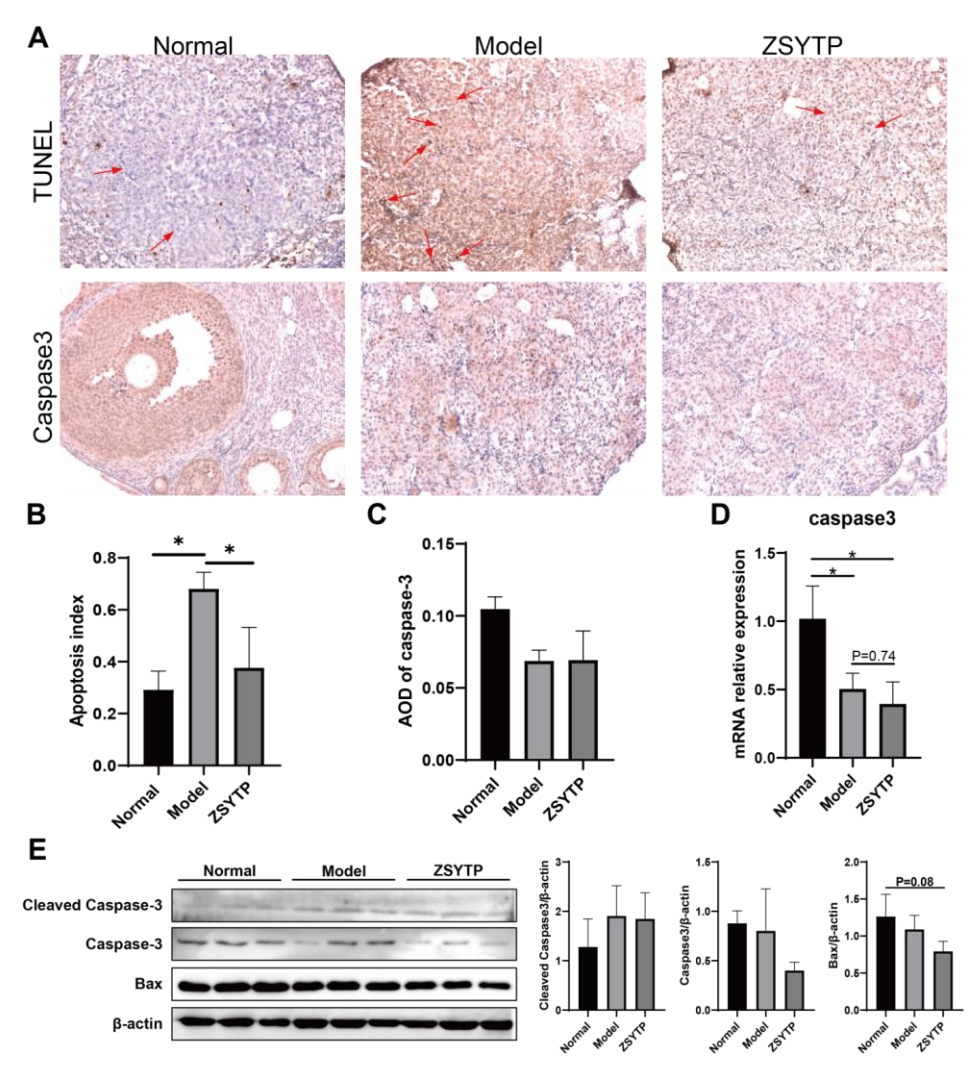


**Figure 3.** Ovarian apoptosis assessment: **(A)** TUNEL staining and immunohistochemical staining of caspase-3 in mice ovaries. Red arrows indicate representative TUNEL-positive cells; **(B)** apoptotic index; **(C)** Average optical density (AOD) of caspase-3; **(D)** caspase-3 expression among three groups; **(E)** Western bloting analysis of Bax, Caspase-3 and cleaved Caspase-3 expression. AOD = IntDen/Area. \**p*-value < 0.05.

During the process of cell apoptosis, caspase-3 is activated as an executor to mediate proteolysis, carrying an essential role in the regulation of apoptosis [30]. Our immunohistochemical staining result indicated no significant difference in caspase-3 level among all three groups, which was consistent with our previous study but inconsistent with other reports [23,26,31] (**Figure 3C**). However, despite no statistical difference, the level of caspase-3 in the Normal group was slightly higher than the other two groups. Results of RT-qPCR further verified this (*p*-value < 0.05; **Figure 3D**). Western blot analysis further confirmed that the expression levels of caspase-3 and its cleaved form did not differ significantly among the three groups, whereas the apoptotic protein Bax exhibited the lowest expression in the ZSYTP group (*p*-value = 0.08; **Figure 3E**). These observations suggest that ZSYTP attenuates ovarian cell apoptosis, yet this effect may not be reflected in whole-ovary apoptosis protein levels.

# 3.4. Differentially expressed genes analysis and functional enrichment analysis

The statistics of RNA sequencing data are shown in **Table S2**. 1935 DEGs existed between the Model and Normal group, containing 1049 up- and 886 down-regulated. Between Model and ZSYTP group, 2137 DEGs included 573 upregulated and 1564 downregulated. 25 common DEGs with most significant upregulated or downregulated ratio across two comparisons were displayed in the combined volcano plots (**Figure 4B,C**). Detailed information was provided in **Table S3**.

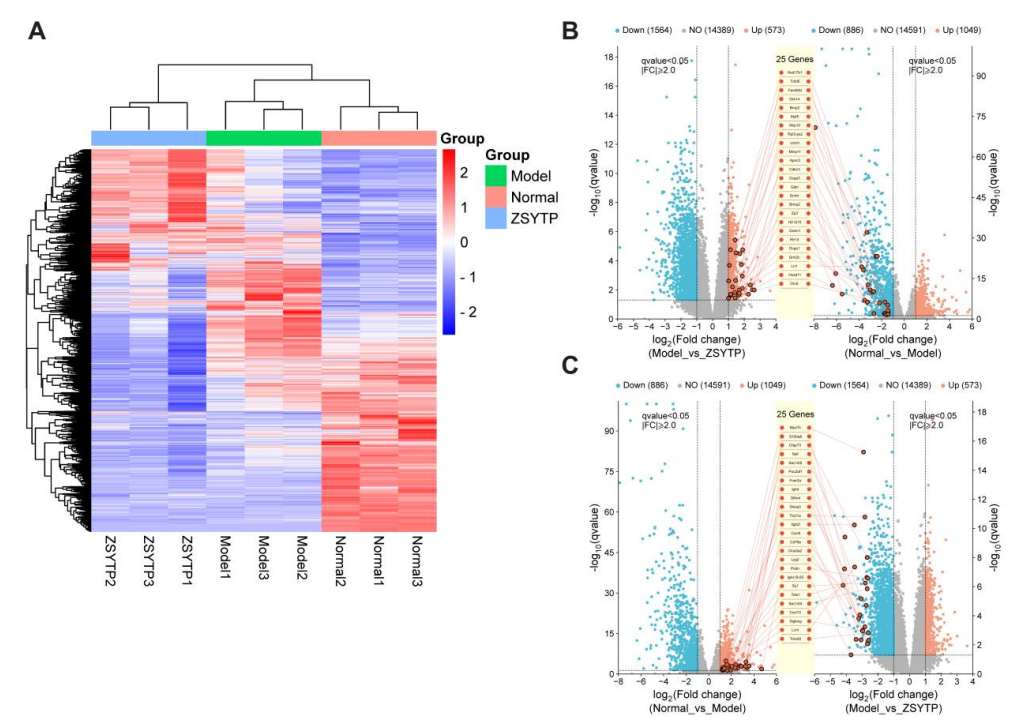


**Figure 4.** DEGs analysis among Normal, Model and ZSYTP group: **(A)** Heatmap of total DEGs expression among three groups; **(B)** Combined Volcano plots of Normal\_vs\_Model DEGs and Model\_vs\_ZSYTP DEGs displayed TOP25 both VCD-upregulated and ZSYTP-downregulated DEGs; **(C)** Combined Volcano plots of Normal\_vs\_Model DEGs and Model\_vs\_ZSYTP DEGs displayed TOP25 both VCD-downregulated and ZSYTP-upregulated DEGs. *q*-value < 0.05, Fold change > 2.

The DEGs of Normal vs. Model comparison and Model vs. ZSYTP comparison were further subjected to GO function enrichment analysis. The top 10 significantly enriched GO entries in biological process (BP), molecular function (MF) and cell component (CC) are displayed (**Figure 5A, D**). As shown in **Figure 5A**, several BPs related to cell proliferation were included, such as cell cycle, cell differentiation and cell division, indicating that VCD exposure disturbed follicular growth in the ovary, which may be mediated by signal transduction. In contrast, although shared several BPs, DEGs between Model and ZSYTP group were mainly involved in GO terms related to transcription and translation, implying that ZSYTP may mitigate VCD-induced POF by regulating gene and protein expression (**Figure 5D**).

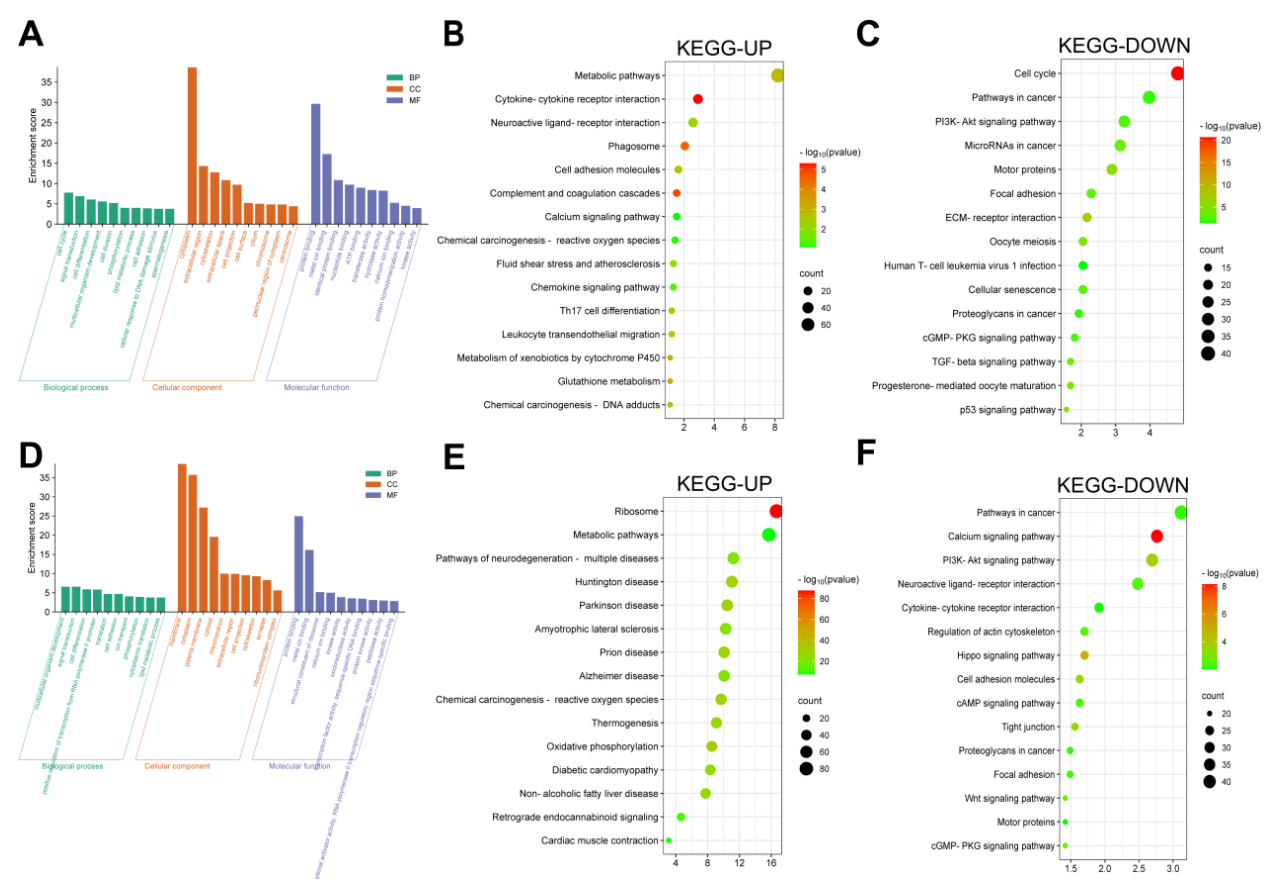


**Figure 5.** GO and KEGG analysis of DEGs: (**A**) GO enrichment analysis of DEGs between Model and Normal group; (**B**) KEGG analysis of upregulated DEGs between Model and Normal group; (**C**) KEGG analysis of downregulated DEGs between Model and ZSYTP group; (**D**) GO enrichment analysis of DEGs between Model and ZSYTP group; (**E**) KEGG analysis of upregulated DEGs between Model and ZSYTP group; (**F**) KEGG analysis of downregulated DEGs between Model and ZSYTP group.

To further find the core pathways in ZSYTP against POF, up- and downregulated DEGs were subjected to KEGG enrichment analysis respectively. Compared with Normal group, upregulated genes in the Model group were significantly enriched in various immune-related pathways (Figure 5B). Besides, metabolic pathways, phagosome, cell adhesion molecules, and calcium signaling pathway were also enriched, indicating diverse mechanism of POF development. As expected, downregulated DEGs in Normal vs. Model comparison were enriched in cell proliferation and development-related terms, including cell cycle, oocyte meiosis, progesteronemediated oocyte maturation, further validating the successful modeling of POF mice (**Figure 5C**). However, cellular senescence was also significantly enriched. Moreover, the four enriched signaling pathways also function in cell proliferation and apoptosis, suggesting a complex mechanism of POF development, upregulated DEGs between Model and ZSYTP group were mostly enriched in ribosome and metabolic pathways, indicating a positive regulation of gene expression and metabolism (Figure 5E). Several enriched pathways of downregulated DEGs in Model vs. ZSYTP comparison, such as calcium signaling pathway and cytokine-cytokine receptor interaction, were shared with upregulated DEGs in Normal vs. Model comparison, which may explain the therapeutic mechanism of ZSYTP (Figure 5F). Other signaling pathways, including PI3K-Akt, Hippo, cAMP, Wnt and cGMP-PKG, were significantly enriched as well. (**Table S4**)

# 3.5. ZSYTP reverse the VCD-induced overactivation of immune response in ovaries

Based on results of KEGG analysis, we intend to explore further those enriched immune-related pathways and verify the consequence of RNA-Seq. Gene Set Enrichment Analysis (GSEA) revealed that VCD exposure caused significant enrichment in immune response pathways and genes, while ZSYTP administration counteracted this immune upregulated tendency (Figure 6A, B). The core genes in regulating immune function of ovary among three groups were exhibited in Figure **6C**. To validate our results, the expression level of s100a8, cxcl13, and cxcl5, were analyzed by RT-qPCR. Although no statistical significance, ovaries from the Model group showed much higher expression level of these three immune-related genes than other groups (**Figure 6D–F**). In addition, the expression of *IL-17A* and *IL-17F* were also assessed to further verify the role of Th17 immune response and IL-17 signaling pathway in the treatment of ZSYTP against POF. Results indicated that ZSYTP significantly decreased the elevated mRNA expression level of IL-17A caused by VCD, whereas no effect on IL-17F expression (Figure 6H, I). These findings confirmed that the overactivation of immune response participates in the pathogenesis of POF, which can be mitigated by ZSYTP.

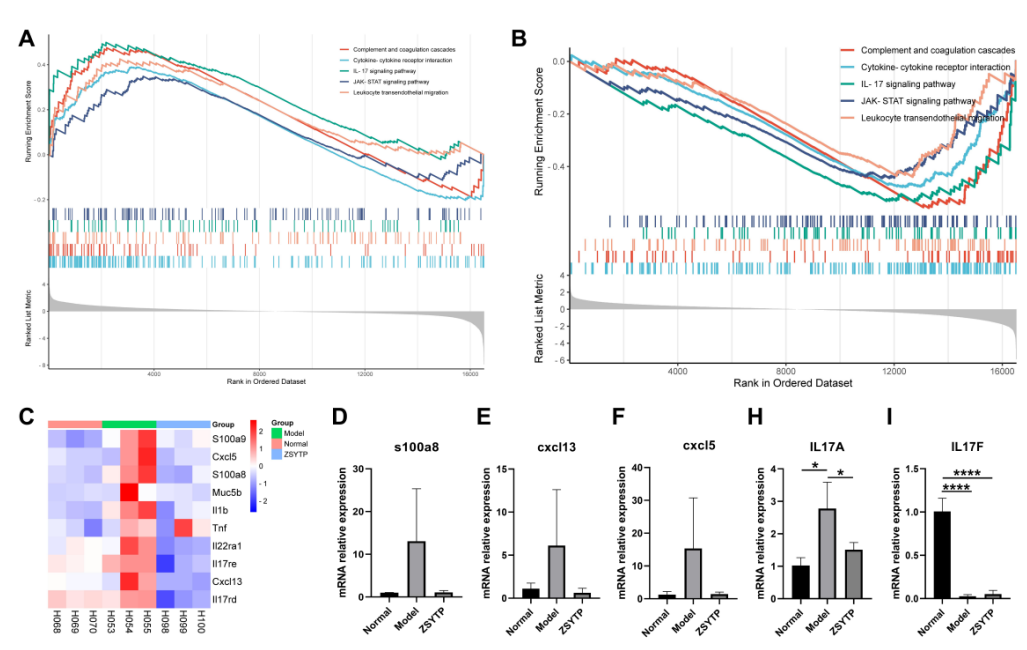


**Figure 6.** GSEA and immune-related gene expression quantification: **(A)** GSEA of KEGG pathways between Model and Normal group; **(B)** GSEA of KEGG pathways between Model and ZSYTP group; **(C)** Heatmap of hub immune-related gene expression level among Normal group, Model group, and ZSYTP group; **(D–I)** RT-qPCR results of immune-related genes.

#### 4. Discussion

TCM has long been employed across Asian countries to treat gynecological disorders, including POF [14]. As a Chinese patent medicine, ZSYTP has been used for years in clinical practices to treat reproductive pathologies, especially infertility [32,33]. Clinical studies demonstrate that ZSYTP ameliorates hormone imbalance symptoms by elevating serum FSH and LH levels, underscoring its therapeutic potential in POF treatment [15,34]. However, its precise therapeutic mechanisms remain to be elucidated.

In this study, we investigated the effects and mechanisms of ZSTYP in a VCD-induced POF mouse model. POF is characterized pathologically by diminished follicles counts at various developmental stages and increased atretic follicles. In clinical practice, elevated FSH levels and reduced AMH levels are key diagnostic markers. Therefore, we first confirmed the successful POF modeling through serum hormone assays and histopathological evaluation of ovarian tissue: two weeks VCD exposure induced hormone perturbations and ovarian histopathological changes consistent with POF (**Figure 2A, B**) (**Figure 3A–F**). Selectively accelerated apoptosis in small ovarian follicles has been regarded as one of the possible mechanisms of VCD-induced POF [19,23,24]. Although TUNEL assay indicated an elevated level of apoptosis in the Model group, caspase-3 expression was unexpectedly downregulated-contrary to previous studies [23,31]. This discrepancy may arise from the difference in stastical method, as we analyzed the whole ovary, while previous study detected caspase-3 upregulation selectively in primordial and small primary follicles following VCD exposure.

To further understand the molecular mechanism of POF and identify the potential therapeutic targets of ZSYTP, DEG analysis was performed based on RNA-Seq data. GO function and KEGG pathway enrichment analysis highlighted that VCD exposure predominantly perturbs cell cycle, cell differentiation, lipid metabolic process, and cell adhesion. Notably, for the first time we discovered a marked overactivation of ovarian immune responses after VCD exposure. The upregulated immune-related pathways covered a wide range, including cytokine-cytokine receptor interaction, complement and coagulation cascades, chemokine signaling pathway, Th17 cell differentiation, and leukocyte transendothelial migration. GSEA results further confirmed enrichment of immune-related pathways, including IL-17 and JAK-STAT signaling pathway, in the Model group compared to both Normal and ZSYTP groups. These findings suggest that the VCD-induced POF model precisely recapitulates immune dysregulation characteristic of POF and that ZSYTP administration can partially reverse these immune perturbations [35,36]. This is the first report demonstrating immune modulation as a mechanism for ZSYTP to treat POF.

Among all the enriched immune-related pathways, IL-17 signaling pathway caught our attention. IL-17, a pro-inflammatory cytokine predominantly produced by Th17 cells, amplifies inflammation by recruiting neutrophils and enhancing production of downstream cytokines and chemokines [37–39]. Elevated IL-17 levels in POF patients imply that Th17-mediated immune responses contribute to ovarian tissue damage [40]. The chronic IL-17-mediated inflammation can increase ovarian cell apoptosis, disrupt follicular development, and ultimately precipitate ovarian failure. Moreover, several studies demonstrate that modulating Th17/Treg balance or

IL-17A/IL-6 axis ameliorates POF, highlighting the IL-17 signaling pathway as a promising therapeutic target [41–43].

JAK-STAT pathway is also deeply involved in immune regulation, governing the differentiation of various T helper cell subsets, including Th1, Th2, and Th17 cells. STAT1 and STAT2 mediate antitumor immunity via type I and II interferons, while STAT3 supports cancer cell survival, immunosuppression, and sustained inflammation [44]. Crucially, STAT3 cooperates with the transcription factor RORγt to drive IL-17 production, the signature cytokine of Th17 cells [45]. Furthermore, JAK-STAT signaling is conserved in granulosa cell across mouse, horse and human ovaries. Inhibition of JAK1 in granulosa cell elevates STAT3 mRNA levels and accelerates primordial follicle activation and apoptosis [46–48]. Together, both the IL-17 and JAK-STAT pathways are key mediators of immune dysfunction in POF, offering promising targets for novel therapeutic strategies.

Based on the enriched gene sets in the Model group and our DEG analysis, we identified candidate hub genes that were upregulated in the Model group yet downregulated in both Normal and ZSYTP groups, with a particular focus on Th17-related factors. Th17 cell mainly secrete IL-17 family cytokines, especially IL-17A and IL-17F, to mediate inflammation and immune response [49]. Our mRNA expression data revealed that ZSYTP significantly attenuated Th17 overactivation via suppression of IL-17A rather than IL-17F, providing direct evidence of the regulating effect of ZSYTP in Th17 function and IL-17 signaling pathway (**Figure 6H, I**).

Among downstream effectors, S100A8 and S100A9 (calprotectin) mediate inflammation by engaging receptors such as TLR4 and activating pathways that promote inflammation, such as NF-κB and MAPK pathways [50]. In the context of Th17 immune responses, S100A8 and S100A9 are known to be upregulated by IL-17, amplifying inflammation in disorders like psoriasis and autoimmune arthritis [51,52]. CXCL13 recruits immune cells and promotes tertiary lymphoid structure formation in chronic inflammation and cancer; it also modulates the Th17/Treg balance [53–55]. CXCL5, a neutrophil chemoattractant induced by IL-17, further perpetuates the inflammatory milieu [56,57]. We selected these three genes for RT-qPCR validation. However, one Model-group sample (H053) diverged markedly from the others, as reflected in both the heatmap and RT-qPCR data (**Figure 6C–F**). This may explain the unexpectedly nonsignificance in RT-qPCR results.

#### 5. Conclusion

In summary, our study showed that ZSTYP could effectively protect mice ovarian function against VCD exposure via various pathways, including calcium, Hippo and cAMP signaling pathway. Among them, downregulation of VCD-induced immune overactivation may be a critical therapeutic mechanism of ZSYTP, marking the first time this has been identified. However, limitations inevitably exist in this study. Due to the limited financial support, we used the minimum sample size required to achieve statistical significance and only adopted a single dosage of ZSYTP for intervention. Possibly, this may have affected the accuracy of our results. Besides, due to the complex etiology of POF, more POF models with different pathogenetic mechanisms should be included to test ZSYTP. Besides, different animal models

should also be considered. Hopefully, we expect more studies not only to further investigate the therapeutic effects of ZSYTP on POF, but also to study the other time-honored prescriptions of TCM. We believe with the use of modern science and technology, TCM, an invaluable treasure from our ancestors, will be understood and accepted by people worldwide and benefit them all.

#### **Supplementary materials:**

**Table S1:** The sequences of primers

Table S2: Statistics of RNA-Seq data

**Table S3:** Details of DEGs in RNA-Seq

**Table S4:** Details of GO and KEGG enrichment

**Author contributions:** HJ designed the research study. ZS, KS, JZ and LL conducted the experiment and drafted the original manuscript. ZS and KS performed data analysis. All authors read and approved the final manuscript. All authors have read and agreed to the published version of the manuscript.

**Acknowledgments:** We would like to thank Editage (www.editage.cn) for its linguistic assistance during the preparation of this manuscript.

**Funding:** This study was financed by grant from Luo Yuankai Zishen Yutai Pills Research Fund for young and middle-aged talents (no. 20190505), and Natural Science Foundation of Jiangxi Provincial (no. 20212BAB206026).

**Institutional review board statement:** The animal study protocol was approved by the Institutional Animal Care and Use Committee of Nanchang Royo Biotech Co,. Ltd (IACUC Issue No: RYE20212012601; approved at January 26, 2021)

**Informed consent statement:** Not applicable.

**Conflict of interest:** The authors declare no conflict of interest.

## References

- 1. Nash Z, Davies M. Premature ovarian insufficiency. BMJ; 2024. doi: 10.1136/bmj-2023-077469
- 2. Panay N, Anderson RA, Bennie A, et al. Evidence-based guideline: premature ovarian insufficiency. Human Reproduction Open. 2024; 2024(4): hoae065. doi: 10.1093/hropen/hoae065
- 3. Coulam CB, Adamson SC, Annegers JF. Incidence of premature ovarian failure. Obstet Gynecol. 1986; 67(4): 604-606.
- 4. Sheikhansari G, Aghebati-Maleki L, Nouri M, et al. Current approaches for the treatment of premature ovarian failure with stem cell therapy. Biomedicine & Pharmacotherapy. 2018; 102: 254-262. doi: 10.1016/j.biopha.2018.03.056
- 5. Wang Y, Jiang J, Zhang J, et al. Research progress on the etiology and treatment of premature ovarian insufficiency. Biomedicine Hub. 2023; 8(1): 97-107. doi: 10.1159/000535508
- 6. Armeni E, Paschou SA, Goulis DG, et al. Hormone therapy regimens for managing the menopause and premature ovarian insufficiency. Best Practice & Research Clinical Endocrinology & Metabolism. 2021; 35(6): 101561. doi: 10.1016/j.beem.2021.101561
- 7. Rozenberg S, Di Pietrantonio V, Vandromme J, et al. Menopausal hormone therapy and breast cancer risk. Best Practice & Research Clinical Endocrinology & Metabolism. 2021; 35(6): 101577. doi: 10.1016/j.beem.2021.101577

- 8. Fournier A, Cairat M, Severi G, et al. Use of menopausal hormone therapy and ovarian cancer risk in a French cohort study. JNCI: Journal of the National Cancer Institute. 2023; 115(6): 671-679. doi: 10.1093/jnci/djad035
- 9. Zhang B, Liu J. Clinical research and treatment progress of premature ovarian failure in traditional Chinese and western medicine (Chinese). Modern Journal of Integrated Traditional Chinese and Western Medicine. 2020; 29(32): 3543-648. doi: 10.3969/j.issn.1008-8849.2020.32.025
- 10. Yahyavi Y, Kheradi N, Karimi A, et al. Novel advances in cell-free therapy for premature ovarian failure (POF): A comprehensive review. Advanced Pharmaceutical Bulletin. 2024; 14(3): 543-557. doi: 10.34172/apb.2024.059
- 11. Zhang L, Mao B, Zhao X, et al. Translation regulatory long non-coding RNA 1 (TRERNA1) sponges microRNA-23a to suppress granulosa cell apoptosis in premature ovarian failure. Bioengineered. 2022; 13(2): 2173-2180. doi: 10.1080/21655979.2021.2023802
- 12. Fu YX, Ji J, Shan F, et al. Human mesenchymal stem cell treatment of premature ovarian failure: New challenges and opportunities. Stem Cell Research & Therapy. 2021; 12(1). doi: 10.1186/s13287-021-02212-0
- 13. Yi Y, Ma F, Jiao Y, et al. Comparative efficacy of acupuncture therapies in premature ovarian failure: A systematic review and network meta-analysis. Complementary Therapies in Medicine. 2025; 89: 103141. doi: 10.1016/j.ctim.2025.103141
- 14. He Q, Wan S, Jiang M, et al. Exploring the therapeutic potential of tonic Chinese herbal medicine for gynecological disorders: An updated review. Journal of Ethnopharmacology. 2024; 329: 118144. doi: 10.1016/j.jep.2024.118144
- 15. Pang Z, Liang J, Zhong X, et al. The clinical research on Zishen Yutai Pill in the treatment of diminished ovarian reserve for 300 cases (Chinese). Chinese Medicine Modern Distance Education of China. 2017; 15(24): 43-5. doi:10.3969/j.issn.1672-2779.2017.24.019
- 16. Chen J, Wang N, Peng Z, et al. Zishen Yutai pill ameliorates ovarian reserve by mediating PI3K-Akt pathway and apoptosis level in ovary. Journal of Ovarian Research. 2025; 18(1). doi: 10.1186/s13048-025-01643-0
- 17. Mang X, Cui H, Zhang F. Effect of Zishen Yutai pill on ovarian reserve function and pregnancy outcome in infertile patients (Chinese). Shaanxi Journal of Traditional Chinese Medicine. 2019; 40(02): 198-200. doi: 10.3969/j.issn.1000-7369.2019.02.017
- 18. Li Y, He R, Qin X, et al. Transcriptome analysis during 4-vinylcyclohexene diepoxide exposure-induced premature ovarian insufficiency in mice. PeerJ. 2024; 12: e17251. doi: 10.7717/peerj.17251
- 19. Tran DN, Jung EM, Yoo YM, et al. Depletion of follicles accelerated by combined exposure to phthalates and 4-vinylcyclohexene diepoxide, leading to premature ovarian failure in rats. Reproductive Toxicology. 2018; 80: 60-67. doi: 10.1016/j.reprotox.2018.06.071
- 20. Sen Halicioglu B, Saadat KASM, Tuglu MI. The relationship of 4-vinylcyclohexene diepoxide toxicity with cell death, oxidative stress, and gap junctions in female rat ovaries. Reproductive Medicine and Biology. 2021; 20(4): 543-553. doi: 10.1002/rmb2.12398
- 21. Cao LB, Leung CK, Law PWN, et al. Systemic changes in a mouse model of VCD-induced premature ovarian failure. Life Sciences. 2020; 262: 118543. doi: 10.1016/j.lfs.2020.118543
- 22. Kappeler CJ, Hoyer PB. 4-vinylcyclohexene diepoxide: a model chemical for ovotoxicity. Systems Biology in Reproductive Medicine. 2012; 58(1): 57-62. doi: 10.3109/19396368.2011.648820
- 23. Hu X, Christian PJ, Thompson KE, et al. Apoptosis induced in Rats by 4-Vinylcyclohexene diepoxide is associated with activation of the Caspase Cascades 1. Biology of Reproduction. 2001; 65(1): 87-93. doi: 10.1095/biolreprod65.1.87
- 24. Song W, Qiu YT, Li XZ, et al. 4-vinylcyclohexene diepoxide induces apoptosis by excessive reactive oxygen species and DNA damage in human ovarian granulosa cells. Toxicology in Vitro. 2023; 91: 105613. doi: 10.1016/j.tiv.2023.105613
- 25. Fernandez SM, Keating AF, Christian PJ, et al. Involvement of the KIT/KITL signaling pathway in 4-Vinylcyclohexene diepoxide-induced ovarian follicle loss in Rats1. Biology of Reproduction. 2008; 79(2): 318-327. doi: 10.1095/biolreprod.108.067744
- 26. Song Z, Song K, Zhao H, et al. Network analysis and experimental approach to investigate the potential therapeutic mechanism of zishen yutai pills on premature ovarian insufficiency. Heliyon. 2023; 9(9): e20025. doi: 10.1016/j.heliyon.2023.e20025
- 27. Kim D, Paggi JM, Park C, et al. Graph-based genome alignment and genotyping with HISAT2 and HISAT-genotype. Nature Biotechnology. 2019; 37(8): 907-915. doi: 10.1038/s41587-019-0201-4
- 28. Love MI, Huber W, Anders S. Moderated estimation of fold change and dispersion for RNA-seq data with DESeq2. Genome Biology. 2014; 15(12). doi: 10.1186/s13059-014-0550-8

- 29. Sherman BT, Hao M, Qiu J, et al. DAVID: a web server for functional enrichment analysis and functional annotation of gene lists (2021 update). Nucleic Acids Research. 2022; 50(W1): W216-W221. doi: 10.1093/nar/gkac194
- 30. Asadi M, Taghizadeh S, Kaviani E, et al. Caspase-3: Structure, function, and biotechnological aspects. Biotechnology and Applied Biochemistry. 2021; 69(4): 1633-1645. doi: 10.1002/bab.2233
- 31. Takai Y, Canning J, Perez GI, et al. Bax, Caspase-2, and Caspase-3 Are Required for Ovarian Follicle Loss Caused by 4-Vinylcyclohexene Diepoxide Exposure of Female Mice in Vivo. Endocrinology. 2003; 144(1): 69-74. doi: 10.1210/en.2002-220814
- 32. Zhang Y, Yan W, Ge PF, et al. Study on prevention effect of Zishen Yutai pill combined with progesterone for threatened abortion in rats. Asian Pacific Journal of Tropical Medicine. 2016; 9(6): 577-581. doi: 10.1016/j.apjtm.2016.04.002
- 33. Maharajan K, Xia Q, Duan X, et al. Therapeutic importance of Zishen Yutai Pill on the female reproductive health: A review. Journal of Ethnopharmacology. 2021; 281: 114523. doi: 10.1016/j.jep.2021.114523
- 34. Xie J, Chen M. Clinical effect of Zishen Yutai Pill combined with climen on premature ovarian failure (Chinese). Journal of Hunan University of Chinese Medicine. 2017; 37(12): 1396-1399. doi: 10.3969/j.issn.1674-070X.2017.12.023
- 35. Ma L, Lu H, Chen R, et al. Identification of key genes and potential new biomarkers for ovarian aging: A study based on rna-sequencing data. Frontiers in Genetics. 2020; 11. doi: 10.3389/fgene.2020.590660
- 36. Zhang C, Yu D, Mei Y, et al. Single-cell RNA sequencing of peripheral blood reveals immune cell dysfunction in premature ovarian insufficiency. Frontiers in Endocrinology. 2023; 14. doi: 10.3389/fendo.2023.1129657
- 37. McGeachy MJ, Cua DJ, Gaffen SL. The IL-17 family of cytokines in health and disease. Immunity. 2019; 50(4): 892-906. doi: 10.1016/j.immuni.2019.03.021
- 38. Mills KHG. IL-17 and IL-17-producing cells in protection versus pathology. Nature Reviews Immunology. 2022; 23(1): 38-54. doi: 10.1038/s41577-022-00746-9
- 39. Zhong Z, Su G, Kijlstra A, et al. Activation of the interleukin-23/interleukin-17 signalling pathway in autoinflammatory and autoimmune uveitis. Progress in Retinal and Eye Research. 2021; 80: 100866. doi: 10.1016/j.preteyeres.2020.100866
- 40. Kunicki M, Rzewuska N, Gross-Kępińska K. Immunophenotypic profiles and inflammatory markers in premature ovarian insufficiency. Journal of Reproductive Immunology. 2024; 164: 104253. doi: 10.1016/j.jri.2024.104253
- 41. Hu Y, Zhong R, Guo X, et al. Jinfeng pills ameliorate premature ovarian insufficiency induced by cyclophosphamide in rats and correlate to modulating IL-17A/IL-6 axis and MEK/ERK signals. Journal of Ethnopharmacology. 2023; 307: 116242. doi: 10.1016/j.jep.2023.116242
- 42. Hu F, Zhou X, Jiang Y, et al. Effect of myrcene on Th17/Treg balance and endocrine function in autoimmune premature ovarian insufficiency mice through the MAPK signaling pathway. Protein & Peptide Letters. 2022; 29(11): 954-961. doi: 10.2174/0929866529666220822100604
- 43. Shuai L, She J, Diao R, et al. Hydroxychloroquine protects against autoimmune premature ovarian insufficiency by modulating the Treg/Th17 cell ratio in BALB/c mice. American Journal of Reproductive Immunology. 2023; 89(4). doi: 10.1111/aji.13686
- 44. Owen KL, Brockwell NK, Parker BS. JAK-STAT signaling: A double-edged sword of immune regulation and cancer progression. Cancers. 2019; 11(12): 2002. doi: 10.3390/cancers11122002
- 45. Seif F, Khoshmirsafa M, Aazami H, et al. The role of JAK-STAT signaling pathway and its regulators in the fate of T helper cells. Cell Communication and Signaling. 2017; 15(1). doi: 10.1186/s12964-017-0177-y
- 46. Sutherland JM, Frost ER, Ford EA, et al. Janus kinase JAK1 maintains the ovarian reserve of primordial follicles in the mouse ovary. MHR: Basic science of reproductive medicine. 2018; 24(11): 533-542. doi: 10.1093/molehr/gay041
- 47. Hall SE, Upton RMO, McLaughlin EA, et al. Phosphoinositide 3-kinase/protein kinase B (PI3K/AKT) and Janus kinase/signal transducer and activator of transcription (JAK/STAT) follicular signalling is conserved in the mare ovary. Reproduction, Fertility and Development. 2018; 30(4): 624. doi: 10.1071/rd17024
- 48. Frost ER, Ford EA, Peters AE, et al. Signal transducer and activator of transcription (STAT) 1 and STAT3 are expressed in the human ovary and have Janus kinase 1-independent functions in the COV434 human granulosa cell line. Reproduction, Fertility and Development. 2020; 32(12): 1027. doi: 10.1071/rd20098
- 49. Huangfu L, Li R, Huang Y, et al. The IL-17 family in diseases: from bench to bedside. Signal Transduction and Targeted Therapy. 2023; 8(1). doi: 10.1038/s41392-023-01620-3
- 50. Zhou H, Zhao C, Shao R, et al. The functions and regulatory pathways of S100A8/A9 and its receptors in cancers. Frontiers in Pharmacology. 2023; 14. doi: 10.3389/fphar.2023.1187741

- 51. Koenders MI, Marijnissen RJ, Devesa I, et al. Tumor necrosis factor—interleukin-17 interplay induces S100A8, interleukin-1β, and matrix metalloproteinases, and drives irreversible cartilage destruction in murine arthritis: Rationale for combination treatment during arthritis. Arthritis & Rheumatism. 2011; 63(8): 2329-2339. doi: 10.1002/art.30418
- 52. Christmann C, Zenker S, Martens L, et al. Interleukin 17 promotes expression of alarmins S100A8 and S100A9 during the inflammatory response of keratinocytes. Frontiers in Immunology. 2021; 11. doi: 10.3389/fimmu.2020.599947
- 53. Pan Z, Zhu T, Liu Y, et al. Role of the CXCL13/CXCR5 Axis in Autoimmune Diseases. Frontiers in Immunology. 2022; 13. doi: 10.3389/fimmu.2022.850998
- 54. Yang M, Lu J, Zhang G, et al. CXCL13 shapes immunoactive tumor microenvironment and enhances the efficacy of PD-1 checkpoint blockade in high-grade serous ovarian cancer. Journal for ImmunoTherapy of Cancer. 2021; 9(1): e001136. doi: 10.1136/jitc-2020-001136
- 55. Wu X, Guo J, Ding R, et al. CXCL13 blockade attenuates lupus nephritis of MRL/lpr mice. Acta Histochemica. 2015; 117(8): 732-737. doi: 10.1016/j.acthis.2015.09.001
- Wu L, Awaji M, Saxena S, et al. IL-17–CXC chemokine receptor 2 axis facilitates breast cancer progression by upregulating neutrophil recruitment. The American Journal of Pathology. 2020; 190(1): 222-233. doi: 10.1016/j.ajpath.2019.09.016
- 57. Novitskiy SV, Pickup MW, Gorska AE, et al. TGF-β receptor II loss promotes mammary carcinoma progression by Th17-dependent mechanisms. Cancer Discovery. 2011; 1(5): 430-441. doi: 10.1158/2159-8290.cd-11-0100